

Structured Compressed Sensing Based Narrowband Interference Elimination for In-Home Power Line Communications

Sicong Liu, *Student Member*, IEEE, Fang Yang, *Senior Member*, IEEE, Wenbo Ding, *Student Member*, IEEE, Jian Song, *Fellow*, IEEE, and Andrea M. Tonello, *Senior Member*, IEEE

Abstract—The structured compressed sensing based framework for the estimation of NarrowBand Interference (NBI) in power line communication is proposed, which facilitates in-home interconnection and prevents the wired consumer electronics devices from contamination of NBI. To recover the NBI accurately, the Structured Compressed Sensing (SCS) theory is introduced, and the method of SCS based Temporal Differential Measuring (SCS-TDM) is proposed, which fully exploits the temporal correlation of NBI. By exploiting the repeated training sequences, the NBI measurements matrix is acquired. With the exploitation of the prior partial support information, a more effective greedy algorithm, structured prior aided sparsity adaptive matching pursuit, is proposed. The performance of the proposed algorithm is theoretically guaranteed, and simulation results validate that the proposed method significantly outperforms existing counterparts.

Index Terms— In-home interconnection, power line communications, narrowband interference, structured compressed sensing.

I. INTRODUCTION

POWER Line Communication (PLC) systems are attracting considerable attention to implement efficient and low-cost

in-home interconnection, Internet of Things (IoT), and smart home consumer electronics applications [1], [2]. This is because PLC provides connectivity without new dedicated wires by exploiting in-home or in-building electrical distribution grid, thus significantly reducing the deployment costs for the interconnections between wired consumer electronics devices [3], [4]. In PLC, the commonly adopted transmission technology is based on Orthogonal Frequency Division Multiplexing (OFDM). Both the International Telecommunications Union (ITU) G.9960 standard and the IEEE 1901 standard have adopted OFDM transmission to overcome the frequency-selective fading introduced by the propagation medium, and improve spectral efficiency [5], [6]. Compared with other mediums, an important characteristic of power lines is that there exist severe noise and interference [7]. Specifically, NarrowBand Interference (NBI) is generated by amateur radio and radio broadcasting signals coupling into the grid. NBI has a stochastic nature and a sparse spectrum within the wide operating band, i.e. 2-80 MHz used by broadband PLC systems. NBI in power lines is usually much more intensive than that in wireless channels [8] due to various interferer sources and stronger intensity in power line environments. NBI in power lines causes severe degradation to the performance of the receiver, particularly synchronization as analyzed by Marey and Steendam [8], and demodulation investigated by Meng [9].

To mitigate NBI, several schemes have been proposed. A time-frequency interleaving scheme is combined with channel coding to exploit diversity and mitigate NBI [10]. Frequency Threshold Excision (FTE) is used by Kai *et al.* [11], which consists of detecting and excluding the OFDM sub-carriers with power larger than a certain threshold. Soft feedback from the decoding unit is used in a successive NBI cancellation method for OFDM systems by Darsena [12], although errors in the NBI estimation might spread into a number of OFDM sub-carriers. Through the aid of virtual sub-carriers and Linear Minimum Mean Square Error (LMMSE) estimation, the NBI can be subtracted from the received signal if the virtual sub-carriers are near the NBI contaminated sub-carriers as studied by Nilsson *et al.* [13].

However, conventional methods suffer from data loss, error propagation or lack of exact prior information, which results in performance limitation and inevitable inaccuracy of estimation.

Manuscript received December 2, 2016; accepted February 28, 2016. Date of publication April 12, 2017. This work was supported by the Natural Science Foundation of China (Grant No. 61401248), the New Generation Broadband Wireless Mobile Communication Network of the National Science and Technology Major Projects (Grant No. 2015ZX03002008), Science and Technology Project of State Grid Corporation of China (Grant No. SGHAZZ00FCJS1500238), and the Tsinghua University Initiative Scientific Research Program (Grant No. 2014Z06098). (*Corresponding author: Fang Yang.*)

S. Liu is with Electronic Engineering, Tsinghua University, Beijing 100084, P. R. China (email: liu-sc12@mails.tsinghua.edu.cn).

F. Yang is with Research Institute of Information Technology, Tsinghua University, Beijing 100084, P. R. China (email: fangyang@tsinghua.edu.cn).

W. Ding is with Electronic Engineering, Tsinghua University, Beijing 100084, P. R. China (email: dwb11@mails.tsinghua.edu.cn).

J. Song is with Electronic Engineering Department, Tsinghua University, Beijing 100084, P. R. China (email: jsong@tsinghua.edu.cn).

A. M. Tonello is with the University of Klagenfurt, 9020 Klagenfurt, Austria (email: andrea.tonello@aau.at).

F. Yang and J. Song are also with Key Laboratory of Digital TV System of Guangdong Province and Shenzhen City, Shenzhen 518057, P. R. China.

Color versions of one or more of the figures in this paper are available online at <http://ieeexplore.ieee.org>.

Digital Object Identifier 10.1109/TCE.2017.014667

The Compressed Sensing (CS) theory can be used to recover the NBI signal, which stems out of the observation that the NBI is sparse in the frequency domain. The CS theory claims that a sparse signal can be accurately reconstructed from the measurement data with much smaller size than the signal dimension in the presence of background noise [14]. However, the research on CS-based NBI estimation for OFDM-based PLC systems with training preamble is insufficient.

An important aspect when incorporating CS is how to acquire the measurement data of the NBI, since the NBI is mixed up with the information data or training sequences. In the authors' preliminary work [15], the Temporal Differential Measurement (TDM) method was proposed to acquire one measurement vector of the NBI from the received repeated Training Sequences (TS) adopted in the PLC standards [5], [6]. Then, the measurement vector is processed by a classical CS algorithm, Sparsity Adaptive Matching Pursuit (SAMP) [16], to estimate the NBI. However, the inherent temporal correlation between the consecutive NBI signals has not yet been fully exploited since only a one-dimensional measurement vector is used. Hence, only a local solution of the NBI is found, rather than a universally optimal estimation of the NBI signal over the whole received frame.

In order to further improve the performance, the authors' previous work [15] is significantly enhanced and improved in this paper. The recently emerging powerful signal processing theory of Structured CS (SCS) [17] is introduced to the area of NBI mitigation for the first time. A SCS-based TDM (SCS-TDM) scheme for NBI recovery is thus proposed, where measurements matrix is constructed from multi-dimensional differential measurement vectors by fully exploiting the temporal correlation, so that a universally optimal solution of the NBI signal over the whole received burst frame can be derived. In detail, the contributions of this paper are as follows.

- The repeating structure of the training preamble specified in PLC systems is fully exploited. The SCS-TDM method is derived by introducing the recent SCS theory to improve the performance of existing counterparts. Multiple temporal differential measurement vectors are used to derive the multi-dimensional measurements matrix, and then the convex optimization framework based on the mixed $l_{1,2}$ -norm minimization is devised.
- A novel SCS-based greedy algorithm, Structured Prior Aided SAMP (SPA-SAMP), is proposed to improve the classical CS algorithm SAMP. SPA-SAMP is able to effectively improve the accuracy and reduce the complexity in estimating the NBI with low Interference-to-Noise Ratio (INR) or large sparsity levels. It is also more applicable for realistic NBI signals than the existing SCS algorithm, Simultaneous Orthogonal Matching Pursuit (S-OMP), which requires known sparsity level [18].

The remainder of this paper is organized as follows: The system and NBI models are described in Section II. Section III presents the details of the proposed SCS-TDM method and the SCS greedy algorithm SPA-SAMP for NBI estimation, along with the theoretical analysis. Simulation results are presented in

Section IV to validate the proposed methods, followed by the conclusions.

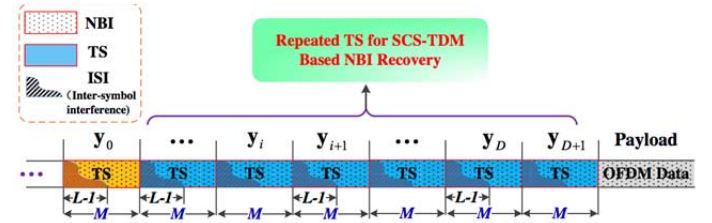


Fig. 1. Received repeated training sequences in the preamble of the G.hn system exploited for SCS-TDM based NBI recovery.

Notation: Matrices and column vectors are denoted by boldface letters; $(\cdot)^{\dagger}$ and $(\cdot)^H$ denote the pseudo-inversion operation and conjugate transpose; $\|\cdot\|_r$ represents the l_r -norm operation; $|\Omega|$ denotes the cardinality of the set Ω ; $\mathbf{v}|_{\Omega}$ denotes the entries of the vector \mathbf{v} in the set of Ω ; $(\mathbf{A})_{i,j}$ denotes the entry at the i -th row and j -th column of matrix \mathbf{A} ; \mathbf{A}_{Ω} represents the sub-matrix made of the Ω columns of the matrix \mathbf{A} ; Ω^c denotes the complementary set of Ω ; $\text{Max}(\mathbf{v}, T)$ denotes the indices of the T largest entries of the vector \mathbf{v} .

II. SYSTEM MODEL

A. OFDM Based PLC System Model

In OFDM based PLC systems, repeated training sequences are often deployed for synchronization, channel estimation and equalization, such as in the preamble of the G.hn standard [5] and the IEEE 1901 standard [6]. For instance, the total number of repeated training sequences is 7 in the IEEE 1901 standard, and is configurable to be 5, 7, 11, or higher, in the preamble specified by the G.hn standard. In this paper, the repeated training sequences are exploited to acquire the measurement vectors of the NBI. Without loss of generality, repeated training sequences in the preamble of G.hn are illustrated in Fig. 1. The transmitted training sequences are identical and each of them can be denoted by $\mathbf{c} = [c_0, c_1, \dots, c_{M-1}]^T$, where M is the length of each training sequence. The payload data transmitted after the training sequences consist of a certain number of OFDM data blocks.

The received samples corresponding to the i -th received training sequence can be written in vector format as

$$\mathbf{y}_i = \Phi \mathbf{h}_i + \mathbf{e}_i + \mathbf{w}_i = \Phi \mathbf{h}_i + \mathbf{F}_M \tilde{\mathbf{e}}_i + \mathbf{w}_i, \quad (1)$$

where the length- M vector $\mathbf{y}_i = [y_{i,0}, y_{i,1}, \dots, y_{i,M-1}]^T$, $i = 0, 1, \dots, D+1$ denotes the i -th received training sequence, and the total number of repeated training sequences is $D+2$. The system model takes into account the presence of: a) a dispersive PLC channel with the Channel Impulse Response (CIR) $\mathbf{h}_i = [\mathbf{h}_{i,0}, \mathbf{h}_{i,1}, \dots, \mathbf{h}_{i,L-1}]^T$, with $L < M$; b) NBI whose time-domain vector is $\mathbf{e}_i \in \mathbb{C}^M$ and frequency domain vector is $\tilde{\mathbf{e}}_i \in \mathbb{C}^N$, where N is the number of OFDM sub-carriers and $M < N$; c) Additive White Gaussian Noise (AWGN) modeled vector $\mathbf{w}_i \in \mathbb{C}^M$ with i.i.d. components having zero mean and variance σ^2 . The channel is assumed to be time-invariant during the transmission of the repeated training sequences. The training sequence

component at the receiver is represented by $\Phi \mathbf{h}_i$ where the matrix $\Phi \in \mathbb{C}^{M \times L}$ is given by

$$\Phi = \begin{bmatrix} c_0 & c_{M-1} & c_{M-2} & \cdots & c_{M-L+1} \\ c_1 & c_0 & c_{M-1} & \cdots & c_{M-L+2} \\ \vdots & \vdots & \vdots & \ddots & \vdots \\ c_{M-1} & c_{M-2} & c_{M-3} & \cdots & c_{M-L} \end{bmatrix}_{M \times L}. \quad (2)$$

The time-domain NBI is written as $\mathbf{e}_i = \mathbf{F}_M \tilde{\mathbf{e}}_i$ assuming that $\tilde{\mathbf{e}}_i = [\tilde{e}_{i,0}, \tilde{e}_{i,1}, \dots, \tilde{e}_{i,N-1}]^T$ is the vector denoting the NBI in the frequency domain at the OFDM receiver, while $\mathbf{F}_M \in \mathbb{C}^{M \times N}$ is the partial Inverse Discrete Fourier Transform (IDFT) matrix composed of the first M rows of the full $N \times N$ IDFT matrix, which is given by

$$\mathbf{F}_M = \frac{1}{\sqrt{N}} [\gamma_0 \quad \gamma_1 \quad \cdots \quad \gamma_{N-1}], \quad (3)$$

where γ_k is a vector with the n -th element equal to $\exp(j2\pi kn/N)$, $n = 0, 1, \dots, M-1$.

B. Statistical Model of NBI in PLC

The NBI is modeled as the superposition of a number of Band-Limited Gaussian Noise (BLGN) processes as a result of the wireless and broadcasting radio signals coupling into the power grid transmitted in the same spectrum, e.g., in the 2-30 MHz band, [2], [19]–[21]. Since an OFDM transmission system with N sub-carriers is considered (the repeated training sequences length M is configured to be smaller than the OFDM sub-carrier number N in PLC standards, $M < N$), the NBI can be modeled in the frequency domain as a sparse vector $\tilde{\mathbf{e}}_i$ of length N . The time domain NBI signal $\mathbf{e}_i = [e_{i,0}, e_{i,1}, \dots, e_{i,M-1}]^T$ associated to the i -th training sequence is modeled by a superposition of jamming tones as follows

$$e_{i,n} = \sum_{k \in \Omega_i} \tilde{e}_{i,k} \cdot \exp\left(\frac{j2\pi kn}{N}\right), n = 0, 1, \dots, M-1, \quad (4)$$

where $\Omega_i = \{k \mid \tilde{e}_{i,k} \neq 0, k = 0, 1, \dots, N-1\}$ is the frequency domain NBI support, i.e., the set of indices of the nonzero entries. The nonzero entries are in correspondence to the sub-carriers hit by NBI. They are modeled as Gaussian distributed random variables with zero mean and power $\sigma_{e,k}^2, k \in \Omega_i$. The powers of different tone interferers could be random and different from each other since the NBI interferer sources might be different in practice. As previously described, the time domain and frequency domain NBI vectors are related by the IDFT operation as $\mathbf{e}_i = \mathbf{F}_M \tilde{\mathbf{e}}_i$. The sparsity level K of the NBI vector is defined as the number of nonzero entries and it is much smaller than the signal dimension, i.e. $K = |\Omega_i| \ll N$. The INR ρ can be used as an indicator of the NBI intensity with respect to the background AWGN, which is calculated by

$$\rho = \frac{1}{\sigma^2} \mathbb{E} \left\{ \sum_{k \in \Omega_i} |\tilde{e}_{i,k}|^2 / K \right\}. \quad (5)$$

The locations of the nonzero entries are assumed to be randomly distributed in all the OFDM sub-carriers [20], and the sparsity level can be variable [2].

C. Temporal Correlation of NBI

An important characteristic of the NBI in power lines, which facilitates the proposed method in this paper, is its *temporal correlation*. Generally, the NBI signal in power lines comes from licensed radio services (analog radio and TV broadcasting [22], [23]), amateur radio signals [24], and other electrical or consumer electronics devices (microwave ovens, personal computers [25], [26]) connected in the power network, etc. Such interference signals are narrowband and transmitted at relatively constant frequencies so that the NBI can be assumed to hit the same sub-carriers of the OFDM blocks over a certain period and keep constant over the repeated training sequences of the preamble.

Typically, according to the field tests and experimental observations on power lines in real house/apartments [27], the NBI interferer in power lines has a bandwidth of around 50 - 5000 Hz, resulting in a Coherent Time (CT) of around 200 μs - 20ms. The supportive data are provided by Corts *et al.* [27], where it was reported that in many cases, the NBI signal is stationary during the AC mains cycle (0.02 s) and its level keeps unchanged based on the field tests. Besides, it was shown that the bandwidth of the observed NBI signal does not exceed 5 kHz. As another example, most of the frequency bands of radio amateur signals in Italy have the bandwidth of 200, 500 and 2700 Hz according to the Italy radio regulations, which means that the NBI generated by amateur radio is static over 370 μs - 5 ms.

Compared with the relatively long duration of the NBI, burst transmission frame with much shorter duration is specified in existing PLC standards. For example, ITU-T G.9960 [5] configures 1024 OFDM sub-carriers in the band 2-30 MHz, and the sub-channel has a bandwidth of about 27 kHz, so the OFDM symbol duration will be 36.5 μs . Hence, the narrowband interferer can be regarded as static over many OFDM symbols, and the CT of NBI is normally longer than the duration of the payload and the preamble. Similarly, according to IEEE P1901 standard [6], the payload duration is only 82 μs - 120 μs , and the duration of the preamble composed of repeated training sequences is 51.2 μs . Thus, the total duration of the burst frame is smaller than the CT of NBI.

Consequently, the support and the amplitudes of the frequency domain NBI signal can be regarded as quasi-static over the consecutive repeated training sequences of the PLC preamble. Specifically, the NBI during D consecutive repeated training sequences can be assumed to share the same sparse pattern, i.e. $\Omega_i = \Omega_{i+1} = \dots = \Omega_{i+D-1} = \Omega$, and have almost the same spectral amplitudes, which is defined as the *temporal correlation*.

Due to the temporal correlation, the support of the NBI and its amplitude (i.e. the modulus of the complex frequency domain nonzero entries) remain constant during the repeated training sequences. Thus, the time domain NBI vector at the $(i+1)$ -th training sequence \mathbf{e}_{i+1} equals that at i -th training sequence \mathbf{e}_i delayed by Δl samples, where $\Delta l = M$ is the number of samples between two adjacent training sequences. Hence, the frequency domain NBI vector at $(i+1)$ -th training sequence $\tilde{\mathbf{e}}_{i+1}$ is equal to $\tilde{\mathbf{e}}_i$ with a phase shift, i.e.,

$$\tilde{e}_{i+1,k} = \tilde{e}_{i,k} \exp\left(\frac{j2\pi k \Delta l}{N}\right), \quad k = 0, 1, \dots, N-1. \quad (6)$$

III. STRUCTURED COMPRESSED SENSING FORMULATION AND SOLUTION FOR NBI RECOVERY WITH TEMPORAL DIFFERENTIAL MEASUREMENTS

A. Proposed SCS Formulation for NBI Recovery: SCS-based Temporal Differential Measuring

Classical CS theory proves that a sparse vector $\mathbf{x} \in \mathbb{C}^N$ can be accurately recovered from a noisy measurement vector $\mathbf{y} \in \mathbb{C}^M$ where $M < N$, as long as the sparse vector can be modeled by the sparse representation $\mathbf{y} = \Psi \mathbf{x} + \mathbf{w}$, where Ψ is the $M \times N$ underdetermined observation matrix satisfying Restricted Isometry Property (RIP) and the background noise \mathbf{w} is bounded. The terminology ‘‘sparse’’ means that there are few nonzero entries in \mathbf{x} . Solving this CS problem is to solve the l_0 -norm minimization problem described by $\mathbf{x} = \arg \min_{\mathbf{x} \in \mathbb{C}^N} \|\mathbf{x}\|_0$, such that $\mathbf{y} = \Psi \mathbf{x}$. Although l_0 -norm minimization is NP-hard, it can be convex relaxed [14] [28], and then solved efficiently using CS greedy algorithms, such as Orthogonal Matching Pursuit (OMP) [29], and SAMP [16].

However, an inevitable drawback of the classical CS method is that the inherent mutual correlation between multiple sparse signals is ignored. This would lead to a significant loss of recovery performance, especially under severe conditions such as low INR, large sparsity level, or insufficient amount of measurement data. Hence, in order to improve the performance, the powerful SCS theory [17] can be introduced to NBI recovery. Through fully exploiting the temporal correlation of NBI, a globally optimal solution can be estimated.

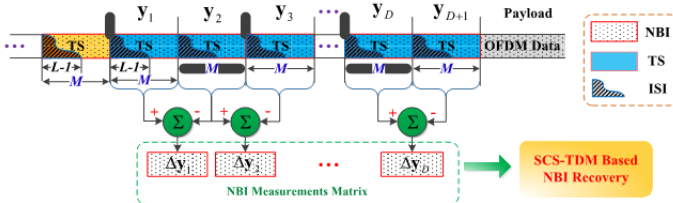


Fig. 2. The SCS-TDM method for NBI recovery using consecutive repeated training sequences in the preamble of the G.hn PLC system.

To apply SCS, it is important to derive appropriate multidimensional measurement data of the signal to be estimated [17]. In fact, the measurement data will contain the NBI component, the AWGN component, and the superimposed training sequence component whose amplitude is much higher than that of AWGN. Hence, it is necessary to null out the training sequence components to ensure successful recovery of NBI. To achieve this goal, as illustrated in Fig. 2, a simple and effective method, referred to as TDM, is capable of acquiring one measurement vector from the repeated training sequences in the preamble. From (1), the training sequence component $\Phi \mathbf{h}_i$ should be canceled in order to acquire the measurement vector, which contains only the NBI and AWGN components. The TDM method simply obtains the measurement vector by a temporal differential operation between two consecutive training sequences. Since the CIR associated with adjacent

training sequences can be regarded as the same, i.e. $\mathbf{h}_i = \mathbf{h}_{i+1}$, the training sequence component are also the same, i.e. $\Phi \mathbf{h}_i = \Phi \mathbf{h}_{i+1}$. Namely, the training sequence component can be eliminated by subtracting \mathbf{y}_{i+1} from \mathbf{y}_i given by (1), yielding a one-dimensional measurement vector $\Delta \mathbf{y}_i$ given by

$$\Delta \mathbf{y}_i = \mathbf{F}_M \Delta \tilde{\mathbf{e}}_i + \Delta \mathbf{w}_i, \quad (7)$$

where $\Delta \mathbf{y}_i = \mathbf{y}_i - \mathbf{y}_{i+1}$, $\Delta \mathbf{w}_i = \mathbf{w}_i - \mathbf{w}_{i+1}$, and the NBI differential vector $\Delta \tilde{\mathbf{e}}_i \in \mathbb{C}^N$ is denoted as

$$\Delta \tilde{\mathbf{e}}_i = \tilde{\mathbf{e}}_i - \tilde{\mathbf{e}}_{i+1} = [\Delta \tilde{e}_{i,0}, \Delta \tilde{e}_{i,1}, \dots, \Delta \tilde{e}_{i,N-1}]^T. \quad (8)$$

Exploiting the temporal correlation in (6), the entries of the NBI differential vector in (8) are given by

$$\Delta \tilde{e}_{i,k} = \tilde{e}_{i,k} \left(1 - \exp\left(j \frac{2\pi}{N} k \cdot \Delta l\right)\right), \quad k = 0, 1, \dots, N-1. \quad (9)$$

Then the SCS theory can be applied by exploiting the $(D+1)$ consecutive received repeated training sequences to constitute the multi-dimensional measurements matrix (as illustrated in Fig.2) and establish the SCS-TDM model given by

$$\Delta \mathbf{Y} = [\Delta \mathbf{y}_1, \Delta \mathbf{y}_2, \dots, \Delta \mathbf{y}_D]_{M \times D} = \mathbf{F}_M \Delta \tilde{\mathbf{E}}_0 + \Delta \mathbf{W}, \quad (10)$$

where $\Delta \tilde{\mathbf{E}}_0 = [\Delta \tilde{\mathbf{e}}_1, \Delta \tilde{\mathbf{e}}_2, \dots, \Delta \tilde{\mathbf{e}}_D]$ is the NBI sparse matrix whose columns share the same support Ω due to the temporal correlation, and the nonzero values in the same row are different from each other by only a phase shift. $\Delta \mathbf{W} = [\Delta \mathbf{w}_1, \Delta \mathbf{w}_2, \dots, \Delta \mathbf{w}_D]$ is the AWGN matrix.

From the measurements matrix in (10), the SCS theory can be precisely applied. Each column of the measurements matrix $\Delta \mathbf{Y}$ is a one-dimensional measurement vector of the NBI corresponding to one pair of adjacent training sequences. The multiple NBI signals within $\Delta \tilde{\mathbf{E}}_0$ that are jointly sparse can be simultaneously recovered by solving the nonlinear SCS optimization problem as follows

$$\Delta \hat{\mathbf{E}} = \arg \min_{\Delta \tilde{\mathbf{E}} \in \mathbb{C}^{N \times D}} \|\Delta \tilde{\mathbf{E}}\|_{0,q}, \quad \text{s.t.} \|\Delta \mathbf{Y} - \mathbf{F}_M \Delta \tilde{\mathbf{E}}\|_{q,q} \leq \varepsilon_S, \quad (11)$$

where ε_S denotes the estimation error bound due to the AWGN noise $\Delta \mathbf{W}$, and the $l_{p,q}$ -norm of a matrix \mathbf{X} is defined as

$$\|\mathbf{X}\|_{p,q} = \left(\sum_m \|(\mathbf{X}^T)_m\|_q^p \right)^{1/p} \quad (12)$$

with $(\mathbf{X}^T)_m$ being the m -th row of \mathbf{X} . The SCS problem in (11) is non-convex when the $l_{0,2}$ -norm is adopted for $\Delta \tilde{\mathbf{E}}$ [17]. Although the $l_{0,q}$ -norm problem (11) is non-convex and NP-hard, it can be relaxed to a convex optimization problem by adopting $l_{p,q}$ -norm of $\Delta \tilde{\mathbf{E}}$ with $p, q \geq 1$ [17]. As the basis of SCS convex optimization methods and BS-MMV methods, the mixed $l_{1,2}$ -norm minimization adopted in this paper can be applied for convex relaxation [30]. Convex relaxing the problem (11) to mixed $l_{1,2}$ -norm minimization yields

$$\Delta \hat{\mathbf{E}} = \arg \min_{\Delta \tilde{\mathbf{E}} \in \mathbb{C}^{N \times D}} \|\Delta \tilde{\mathbf{E}}\|_{1,2}, \quad \text{s.t.} \|\Delta \mathbf{Y} - \mathbf{F}_M \Delta \tilde{\mathbf{E}}\|_{2,2} \leq \varepsilon_S, \quad (13)$$

where the mixed $l_{1,2}$ -norm $\|\Delta \tilde{\mathbf{E}}\|_{1,2}$ is explicitly given by

$$\|\Delta \tilde{\mathbf{E}}\|_{1,2} = \sum_{m=1}^N \|(\Delta \tilde{\mathbf{E}}^T)_m\|_2 \quad (14)$$

with $(\Delta \tilde{\mathbf{E}}^T)_m$ being the m -th row of $\Delta \tilde{\mathbf{E}}$, and thus it can be derived that

$$\varepsilon_s = \|\Delta \mathbf{W}\|_{2,2} = \sqrt{MD\sigma^2}. \quad (15)$$

The existence of the solution to the minimization problem (13) can be theoretically guaranteed. Based on Theorem 2 in the work of Eldar and Mishali [30], it can be further proved that, if the generated block observation matrix $\Psi_B = (\mathbf{F}_M \otimes \mathbf{I}_D)$, with \mathbf{F}_M as given in (10), satisfies the block-RIP with the block-RIP constant $\delta_{2K}^{(B)} < \sqrt{2} - 1$, the estimated NBI matrix $\Delta \hat{\mathbf{E}}$ obtained by solving $l_{1,2}$ -norm minimization (13) is the optimal approximation of the real NBI matrix $\Delta \tilde{\mathbf{E}}_0$ in the noisy measurements given by (10).

Afterwards, the convex mixed $l_{1,2}$ -norm minimization problem (13) can be effectively solved using the SCS greedy algorithm SPA-SAMP as proposed in Section III-B.

B. Enhanced SCS Greedy Algorithm: Structured Prior Aided Sparsity Adaptive Matching Pursuit

SCS greedy algorithms are efficient and effective in estimating the NBI in (13). Unlike classical CS based greedy algorithms that cope with only a one-dimensional measurement vector which is not robust in severe conditions, the algorithm performance can be further improved by exploiting the temporal correlation of multiple repeated training sequences. By maximizing the accuracy of the updated support in the greedy iterations, the SCS greedy algorithm, i.e. SPA-SAMP, is proposed as follows.

Firstly, due to the temporal correlation of NBI, it is possible to acquire and estimate such a prior partial support $\Omega_i^{(0)}$ associated with the i -th training sequence. By exploiting R consecutive differential measured NBI vectors ($R \leq D$), the prior partial support is derived as follows

$$\Omega_i^{(0)} = \{k : \sum_{j=i}^{i+R-1} |\Delta \tilde{y}_{j,k}|^2 > \eta_{th}\}^{N-1}, \quad (16)$$

where $\Delta \tilde{y}_i = [\Delta \tilde{y}_{i,0}, \Delta \tilde{y}_{i,1}, \dots, \Delta \tilde{y}_{i,N-1}]$ is the N -point DFT of $\Delta \mathbf{y}_i$, and the power threshold η_{th} is given by

$$\eta_{th} = \frac{\alpha}{N} \sum_{k=0}^{N-1} \sum_{j=i}^{i+R-1} |\Delta \tilde{y}_{j,k}|^2, \quad (17)$$

where α is a coefficient that can be appropriately chosen according to the scenario. Afterwards, the prior partial support $\Omega_i^{(0)}$ could be exploited to facilitate the initialization and iterations of SPA-SAMP.

The SPA-SAMP algorithm is aimed at solving the relaxed convex SCS optimization problem (11) by using the $l_{1,2}$ -norm of $\Delta \hat{\mathbf{E}}$. The pseudo-code of SPA-SAMP is summarized in **Algorithm 1**. The input to the algorithm includes the measurements matrix $\Delta \mathbf{Y}$, the observation matrix $\Psi = \mathbf{F}_M$, the prior partial support $\Omega^{(0)} = \Omega_i^{(0)}$ acquired from (16), and the iteration step size s that plays a role as a compromise between the convergence rate and the accuracy. The prior support $\Omega^{(0)}$ is exploited to reduce the number of iterations compared to conventional SAMP [16]. The accuracy of the temporary support estimation Ω_t is improved at each iteration, and the testing sparsity level T is increased by s when the stage switches. The halting condition is determined by the $l_{2,2}$ -norm

of the residual matrix $\|\mathbf{R}\|_{2,2} \leq C_\varepsilon \cdot \varepsilon_s$ with

$C_\varepsilon = 1 + \sqrt{1 + \delta_{2K}^{(B)}} \cdot \frac{1 + \delta_{3K} + \delta_{3K}^2}{\delta_{3K}(1 - \delta_{3K})}$, where δ_{3K} and $\delta_{2K}^{(B)}$ denote the RIP and block-RIP constants, respectively. The output of **Algorithm 1** is the final support Ω_S and the recovered NBI matrix $\Delta \hat{\mathbf{E}}$, s.t. $\Delta \hat{\mathbf{E}}|_{\Omega_S} = \Psi_{\Omega_S}^\dagger \Delta \mathbf{Y}, \Delta \hat{\mathbf{E}}|_{\Omega_S^c} = \mathbf{0}$.

Algorithm 1 SPA-SAMP: Structured Prior Aided Sparsity Adaptive Matching Pursuit

Input:

- 1) Prior estimated support $\Omega^{(0)}$
- 2) Initial sparsity level $K^{(0)} = |\Omega^{(0)}|$
- 2) Measurements matrix $\Delta \mathbf{Y}$
- 3) Observation matrix $\Psi = \mathbf{F}_M$
- 4) Step size s .

Initialization:

- 1: $\Delta \hat{\mathbf{E}}^{(0)}|_{\Omega^{(0)}} \leftarrow \Psi_{\Omega^{(0)}}^\dagger \Delta \mathbf{Y}$
- 2: $\mathbf{R}^{(0)} \leftarrow \Delta \mathbf{Y} - \Psi \Delta \hat{\mathbf{E}}^{(0)}$
- 3: $T \leftarrow K^{(0)} + s, k \leftarrow 1$

Iterations:

4: Repeat

- 5: $\mathbf{v} \in \mathbb{C}^N, \text{ s.t. } v_i = \sum_{j=1}^D |(\Psi^H \mathbf{R}^{(k-1)})_{i,j}|$
 - 6: $S_k \leftarrow \text{Max}\{v, T - K^{(0)}\}$ {Preliminary Test}
 - 7: $L_k \leftarrow \Omega^{(k-1)} \cup S_k$ {Make Candidate List}
 - 8: $\mathbf{u} \in \mathbb{C}^{|L_k|}, \text{ s.t. } u_i = \sum_{j=1}^D |(\Psi_{L_k}^\dagger \Delta \mathbf{Y})_{i,j}|$
 - 9: $\Omega_t \leftarrow \text{Max}\{\mathbf{u}, T\}$ {Temporary Final List}
 - 10: $\Delta \hat{\mathbf{E}}^{(k)}|_{\Omega_t} \leftarrow \Psi_{\Omega_t}^\dagger \Delta \mathbf{Y}; \Delta \hat{\mathbf{E}}^{(k)}|_{\Omega_t^c} \leftarrow \mathbf{0}$
 - 11: $\mathbf{R} \leftarrow \Delta \mathbf{Y} - \Psi_{\Omega_t} \Psi_{\Omega_t}^\dagger \Delta \mathbf{Y}$ {Compute Residue}
 - 12: **If** $\|\mathbf{R}\|_{2,2} \geq \|\mathbf{R}^{(k-1)}\|_{2,2}$ **Then**
 - 13: $T \leftarrow T + s$ {Stage Switching}
 - 14: **Else**
 - 15: $\Omega^{(k)} \leftarrow \Omega_t; \Omega_S \leftarrow \Omega_t; \mathbf{R}^{(k)} \leftarrow \mathbf{R}$
 - 16: $k \leftarrow k + 1$ {Same Stage, Next Iteration}
 - 17: **End If**
 - 18: **Until** $\|\mathbf{R}\|_{2,2} \leq C_\varepsilon \cdot \varepsilon_s$
-

Output:

- 1) Final support Ω_S
 - 2) Recovered NBI matrix $\Delta \hat{\mathbf{E}}$ s.t. $\Delta \hat{\mathbf{E}}|_{\Omega_S} = \Psi_{\Omega_S}^\dagger \Delta \mathbf{Y}, \Delta \hat{\mathbf{E}}|_{\Omega_S^c} = \mathbf{0}$
-

It should be observed from **Algorithm 1** that the temporal correlation of NBI is fully exploited in SPA-SAMP. The estimated values of all the D columns of the measurements matrix are summed up to pick the T highest entries in each iteration, instead of making the candidate list from only one measurement vector as in conventional SAMP [16]. Compared to conventional algorithms, SPA-SAMP exhibits better accuracy in support estimation and overall performance as will

be shown in the simulations. Basically, the proposed SPA-SAMP differs from the conventional SAMP in the following two aspects:

Adaptability: The SCS-TDM method exploits the inherent structure of the common support to improve the estimation. Especially in bad conditions that such as small amount of measurements, high background noise or high sparsity levels, SPA-SAMP shows outperforms classical algorithms. The proposed method can also adapt to various sparsity levels, the variation of INR and different length of the measurement vector. Moreover, in case of inaccurate partial support, the structured property and the temporal correlation of NBI will help relieve the inaccuracy and restore the correct final support.

Accuracy: The prior aided initialization in SPA-SAMP is more accurate than the trivial initialization in SAMP. During the stage switching, the testing sparsity level is changed to $T \leftarrow K^{(0)} + j \times s$ instead of $T \leftarrow j \times s$ in SAMP. This makes it possible to adopt a smaller step size s in SPA-SAMP with the same cost of iterations, leading to more accurate estimation of the actual sparsity level K . Besides, the temporal correlation of NBI over D consecutive repeated training sequences is fully utilized by SPA-SAMP. This also leads to more accurate estimation since possible estimation error in one measurement vector can be compensated by the joint recovery process from the multi-dimensional measurements matrix.

The convergence and error performance of SPA-SAMP can be theoretically guaranteed. For convergence, based on the theorems presented by Dai and Milenkovic [31], it can be further proved that, if \mathbf{F}_M satisfies RIP with the constant $\delta_{3K_s} < 0.083$ ($K_s = \lceil K/s \rceil$), the estimated NBI matrix denoted by $\Delta \hat{\mathbf{E}}_{(\ell_{\max})}$ at the end of the final $\ell_{\max} = \lceil K/s \rceil$ -th stage converges to the real NBI $\Delta \hat{\mathbf{E}}_0$ given in (10), with the estimation error bounded by the AWGN power $\|\Delta \mathbf{W}\|_{2,2}$. The total number of iterations of SPA-SAMP N_{IT} is upper bounded by $N_{\text{IT}} \leq \lceil K/s \rceil \cdot (-1.5K_s / \log c_{K_s})$, where $c_{K_s} = 2\delta_{3K_s}(1 + \delta_{3K_s}) / (1 - \delta_{3K_s})^3$. As for error performance, it can be proved that, if the block observation matrix $\Psi_B = (\mathbf{F}_M \otimes \mathbf{I}_D)$ satisfies the block-RIP with block-RIP constant $\delta_{2K}^{(B)} < \sqrt{2} - 1$, the estimation error between the output of SPA-SAMP $\Delta \hat{\mathbf{E}}_{(\ell_{\max})}$ and the solution of the $l_{1,2}$ -norm minimization in (13) $\Delta \hat{\mathbf{E}}$ is upper bounded by ε_s .

C. Final Cancellation of NBI

Until now, the NBI signal over the OFDM data can be recovered and canceled at the receiver. In particular, with the SCS-TDM method, the i -th column of $\Delta \hat{\mathbf{E}}$ is the recovered NBI differential vector $\Delta \hat{\mathbf{e}}_i$ related to the i -th measurement vector $\Delta \mathbf{y}_i$, $i = 1, \dots, D$. Hence, according to the relationship of the phase and amplitude of adjacent NBI signals as indicated by (6), (8), and (9), the original frequency domain NBI vector $\tilde{\mathbf{e}}_i$ associated to the i -th received training sequence \mathbf{y}_i can be accurately reconstructed from $\Delta \hat{\mathbf{e}}_i$ as follows

$$\tilde{\mathbf{e}}_{i,k} = \Delta \hat{\mathbf{e}}_{i,k} / (1 - \exp(j \frac{2\pi k \Delta l}{N})), \quad k = 0, 1, \dots, N-1. \quad (18)$$

Similarly, based on the relationship of the adjacent NBI signals given by (6), the frequency domain NBI vector $\tilde{\mathbf{e}}_n^D = [\tilde{e}_{n,0}^D, \tilde{e}_{n,1}^D, \dots, \tilde{e}_{n,N-1}^D]^T$ associated with the n -th OFDM data block in the payload can be accurately recovered as

$$\tilde{e}_{n,k}^D = \tilde{e}_{i,k} \cdot \exp(j \frac{2\pi k \Delta d_{i,n}}{N}), \quad k = 0, 1, \dots, N-1, \quad (19)$$

where $\{\Delta d_{i,n} = (n-1)P + (D+2-i)M\}_{i=1}^D$ is the number of samples between the i -th received training sequence \mathbf{y}_i and the n -th OFDM data block with the frame length of P as shown by the preamble frame structure in Fig. 1.

Finally, the recovered NBI signal can be canceled from the received OFDM data block. Due to the temporal correlation, the estimation performed during the preamble can be used to be subtracted from the subsequent OFDM data block.

D. Computational Complexity Analysis

The computational complexity of the proposed SCS-TDM method with the SPA-SAMP algorithm is investigated, which is mainly determined by the following three parts:

1) SCS-TDM: the complexity for the acquisition of D measurement vectors is in the order of $\sigma(DM)$.

2) Prior partial support acquisition: the complexity of the prior support acquisition is determined by the DFT of R measurement vectors $\{\Delta \mathbf{y}_j\}_{j=i}^{i+R-1}$ ($\sigma(RN \log_2(N))$) and by the sum and comparisons in (15) ($\sigma(RN)$). Thus the complexity is $\sigma(RN(\log_2(N) + 1))$.

3) SPA-SAMP algorithm: For each iteration, two steps should be considered, i.e., the inner product between the observation matrix and the residue \mathbf{R} with complexity $\sigma(DMN)$ and the equivalent LS problem $\Delta \hat{\mathbf{E}}^{(k)}|_{\Omega} \leftarrow \Psi_{\Omega}^H \Delta \mathbf{Y}$ with complexity $\sigma(DMK)$ since each step is extended to D dimensions. The total number of iterations is reduced from K in SAMP to $K - K^{(0)}$ in SPA-SAMP, so the total complexity of SPA-SAMP is in the order of $\sigma((K - K^{(0)})DM(N + K))$.

To summarize, the overall complexity of the proposed SCS-TDM method with SPA-SAMP algorithm is in the order of $\sigma(RN(\log_2(N) + (K - K^{(0)})DM(N + K)))$. Since the sizes of M , D and K are all sufficiently smaller than N , the complexity is tolerable in practical implementation.

IV. SIMULATION RESULTS AND DISCUSSIONS

In this section, the performance of the proposed NBI recovery method is investigated through computer simulations. The simulation setup is configured according to the typical parameters in the ITU G.hn standard [5]. The OFDM subcarrier number is $N = 1024$ and the length of each training sequence is $M = 128$. For the bit error rate (BER) computation, 64-QAM modulation and the Low Density Parity Check (LDPC) code with code length of 8,640 bits and code rate of 0.5 specified in the ITU G.hn standard [5] are adopted. The PLC multi-path channel model is adopted with the parameters given by Zimmermann and Dostert [32]. As described in Section II, the NBI is modeled by the superposition of independent tone interferers, each with a Gaussian distributed amplitude and an INR = 30 dB in the presence of AWGN. The sparsity level is

invariable for each simulation, and the support is randomly selected in the overall set of N sub-carriers. The coefficient for the prior support acquisition is $\alpha = 6.0$, while the number of consecutive repeated training sequences is $D = 5$. A comparison is made between the proposed SCS-TDM method with the SPA-SAMP algorithm, classical CS methods with SAMP algorithm [15], [16], and conventional FTE [11].

Fig. 3 reports a graphical example of NBI recovery with the classical CS method and the proposed SCS-TDM method assuming $K = 10$ and $\text{INR} = 30$ dB. First, the prior partial support is obtained using the threshold η_{th} given by (17). Then, the measurements matrix of the NBI is acquired through the SCS-TDM method. Finally, the proposed SCS algorithm SPA-SAMP and the classical CS algorithm SAMP are adopted to recover the NBI. It can be observed that the estimation accurately matches the actual NBI very well as shown in Fig. 3.

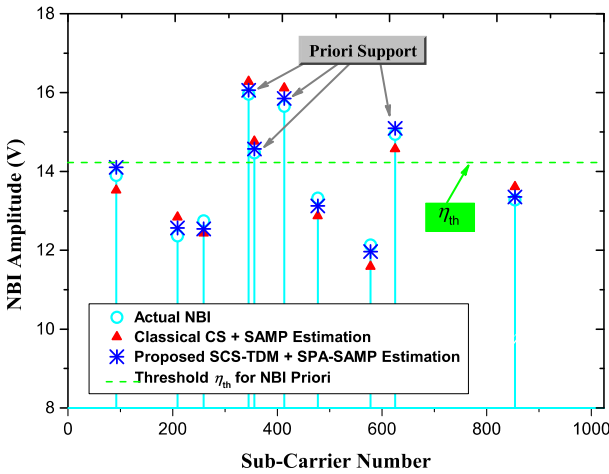


Fig. 3. Graphical visualization of the NBI recovery using the proposed SCS-TDM method with SPA-SAMP algorithm.

The Mean Square Error (MSE) performance of the NBI estimation using the proposed method is shown in Fig. 4. The MSE performance achieved by the proposed SCS-TDM method with SPA-SAMP algorithm, as well as the classical CS method with SAMP algorithm, are both depicted for the sparsity

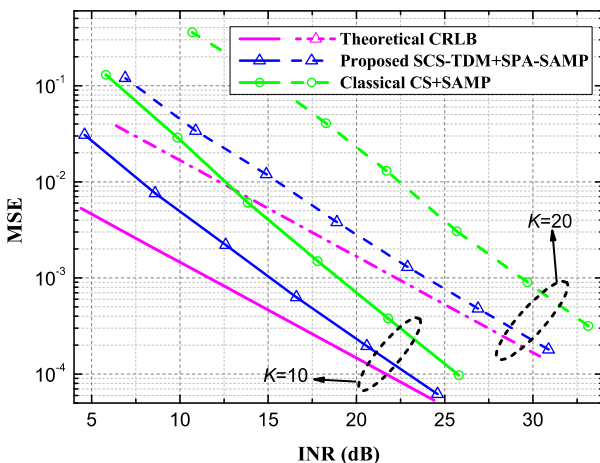


Fig. 4. MSE of the NBI reconstruction using the proposed SCS-TDM method with SPA-SAMP.

sparsity level $K = 10$ and $K = 20$. The theoretical Cramer-Rao Lower Bound (CRLB) that is calculated by $2\sigma^2(K/M)$ is also included as benchmark. The SCS-TDM method with SPA-SAMP algorithm achieves the MSE of 10^{-3} at the INR of 15.1 dB and 23.8 dB for the sparsity levels $K = 10$ and $K = 20$, respectively. It outperforms the classical CS method with SAMP algorithm by approximately 4.9 dB. Furthermore, it is noted from Fig. 4 that the MSE of the proposed methods is approaching the theoretical CRLB as the INR increases.

TABLE I
AVERAGE NUMBER OF ITERATIONS TO REACH SUCCESSFUL NBI RECONSTRUCTION ($\text{MSE} < 10^{-3}$)

Sparsity Level	Proposed SPA-SAMP	Conventional SAMP
10	4.33	8.74
15	7.65	13.53
20	10.18	18.42

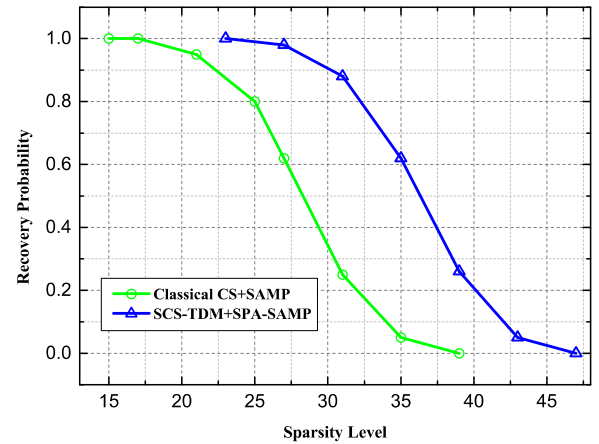


Fig. 5. Probability of NBI recovery using the proposed SCS-TDM method.

The NBI recovery probability is reported in Fig. 5 as a function of the sparsity level K with a fixed INR of 30 dB. The NBI recovery probability is defined as the ratio of the number of successful NBI estimations with $\text{MSE} < 10^{-3}$ over the total number of estimations. It can be noted that the proposed SCS-TDM method with SPA-SAMP algorithm reaches a high recovery probability of 0.9 at the sparsity level of 30, which indicates that the proposed method is capable of correctly recovering the NBI with large sparsity levels from only a small amount of measurement data. It is observed that, the SCS-TDM method with SPA-SAMP algorithm outperforms the classical CS method with SAMP algorithm significantly.

In order to quantitatively compare the execution time (the time complexity) of the proposed SCS algorithm SPA-SAMP and the classical CS algorithm SAMP, the average numbers of iterations using SPA-SAMP and SAMP for NBI recovery are summarized in Table I, where the average value is calculated from 10^6 times of NBI recovery simulations. It can be noted that the average iteration number to reach the same criterion ($\text{MSE} < 10^{-3}$, $\text{INR}=30$ dB) for SPA-SAMP is significantly smaller than that of conventional SAMP with different sparsity levels. Hence, it is indicated from Table I that the time complexity consumed by the proposed SPA-SAMP algorithm

exploiting the temporal correlation, is much lower than that of conventional SAMP.

The BER performance of the proposed SCS-TDM method with SPA-SAMP algorithm as a function of SNR (SNR is calculated at the receiver considering the attenuation introduced by the PLC channel) in the presence of NBI with sparsity level $K = 10$ and INR = 30 dB, is illustrated in Fig. 6. Propagation through the PLC channel and AWGN is also assumed. As baseline performance, the conventional FTE method [11], and the TDM method with classical SAMP algorithm [15], [16] are depicted for comparison. In addition, the worst case where the NBI is not subtracted and the ideal case without NBI are also presented as benchmarks. It can be observed from Fig.6 that, at the target BER of 10^{-4} , the proposed SCS-TDM method with SPA-SAMP algorithm outperforms the classical SAMP algorithm, the conventional FTE method, and the case ignoring NBI by approximately 0.73 dB, 1.34 dB, and 1.67 dB, respectively. Furthermore, Fig. 6 shows that the gap between the proposed SCS-TDM method and the ideal case without NBI is only 0.16 dB, which validates the proposed scheme.

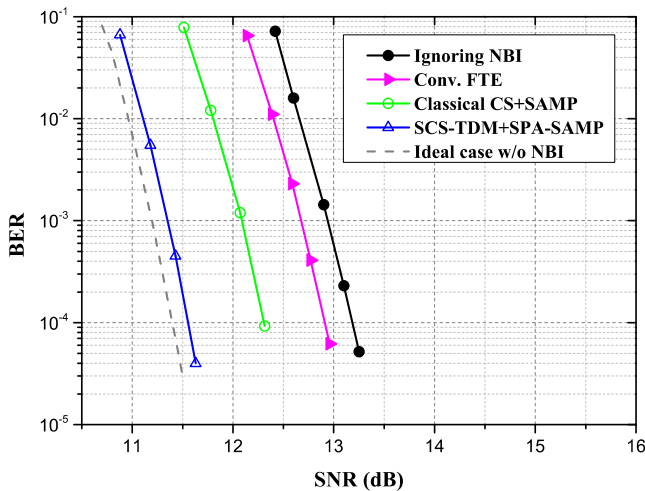


Fig. 6. BER performance comparison of different NBI mitigation schemes.

V. CONCLUSION

In this paper, a novel SCS based scheme in OFDM based low-voltage PLC systems with repeated training sequences was proposed to obtain the multi-dimensional measurements matrix for NBI estimation and cancelation. The prior partial support is acquired and the temporal correlation of NBI is fully exploited by the proposed SPA-SAMP algorithm, whose convergence and error bound can be derived and theoretically guaranteed. The simulation results show that the proposed algorithms are capable of achieving high recovery probability and low MSE in NBI estimation, and lower BER than conventional counterparts. Moreover, the proposed scheme can be easily applied for different communication systems deploying training sequences to estimate and eliminate NBI.

REFERENCES

[1] J. Han, C. S. Choi, W. K. Park, I. Lee, and S. H. Kim, "PLC-based photovoltaic system management for smart home energy management

system," *IEEE Trans. Consum. Electron.*, vol. 60, no. 2, pp. 184–189, 2014.

[2] H. C. Ferreira, L. Lampe, J. Newbury, and T. G. Swart, *Power Line Communications - Theory and Applications for Narrowband and Broadband Communications over Power Lines*. Chichester, UK: Wiley, 2010, pp. 1-6.

[3] M. Korke, N. Hosseinzadeh and T. Moazzeni, "Performance evaluation of a narrowband power line communication for smart grid with noise reduction technique," *IEEE Trans. Consum. Electron.*, vol. 57, no. 4, pp. 1598-1606, Nov. 2011.

[4] J. Han, I. Lee, and S. H. Kim, "User-friendly monitoring system for residential PV system based on low-cost power line communication," *IEEE Trans. Consum. Electron.*, vol. 61, no. 2, pp. 175–180, May 2015.

[5] Unified High-Speed Wire-Line Based Home Networking Transceivers - System Architecture and Physical Layer Specification, ITU-T G.9960 Std., Jun. 2010.

[6] IEEE Standard for Broadband over Power Line Networks: Medium Access Control and Physical Layer Specifications, IEEE 1901-2010 Std., Dec. 2010.

[7] J. Granado, A. Torralba and J. Chavez, "Using broadband power line communications in non-conventional applications," *IEEE Trans. Consum. Electron.*, vol. 57, no. 3, pp. 1092-1098, Aug. 2011.

[8] M. Marey and H. Steendam, "Analysis of the narrowband interference effect on OFDM timing synchronization," *IEEE Trans. Signal Process.*, vol. 55, no. 9, pp. 4558–4566, Sep. 2007.

[9] J. Meng, "Noise analysis of power-line communications using spread spectrum modulation," *IEEE Trans. Power Del.*, vol. 22, no. 3, pp. 1470–1476, Jul. 2007.

[10] S. Liu, F. Yang, and J. Song, "An optimal interleaving scheme with maximum time-frequency diversity for PLC systems," *IEEE Trans. Power Del.*, vol. 31, no. 3, pp. 1007–1014, Jun. 2016.

[11] S. Kai, Z. Yi, B. Kelleci, T. Fischer, E. Serpedin, and A. Karsilayan, "Impacts of narrowband interference on OFDM-UWB receivers: Analysis and mitigation," *IEEE Trans. Signal Process.*, vol. 55, no. 3, pp. 1118–1128, Mar. 2007.

[12] D. Darsena, "Successive narrowband interference cancellation for OFDM systems," *IEEE Commun. Lett.*, vol. 11, no. 1, pp. 73–75, Jan. 2007.

[13] R. Nilsson, F. Sjöberg, and J. LeBlanc, "A rank-reduced LMMSE canceller for narrowband interference suppression in OFDM-based systems," *IEEE Trans. Commun.*, vol. 51, no. 12, pp. 2126–2140, Dec. 2003.

[14] D. Donoho, "Compressed sensing," *IEEE Trans. Inf. Theory*, vol. 52, no. 4, pp. 1289–1306, Apr. 2006.

[15] S. Liu, F. Yang and J. Song, "Narrowband interference cancelation based on priori aided compressive sensing for DTMB systems," *IEEE Trans. Broadcast.*, vol. 61, no. 1, pp. 66-74, Mar. 2015.

[16] T. T. Do, L. Gan, N. H. Nguyen and T. D. Tran, "Fast and efficient compressive sensing using structurally random matrices," *IEEE Trans. Signal Process.*, vol. 60, no. 1, pp. 139-154, Jan. 2012.

[17] M. Duarte and Y. Eldar, "Structured compressed sensing: from theory to applications," *IEEE Trans. Signal Process.*, vol. 59, no. 9, pp. 4053–4085, Sep. 2011.

[18] J. A. Tropp, "Algorithms for simultaneous sparse approximation. part II: convex relaxation," *Signal Process.*, vol. 86, no. 3, pp. 589–602, Mar. 2006.

[19] S. Jagannathan, A. Morales, and S. Agili, "Performance of OFDM-based power line communication under asynchronous noise," in *Proc. ICCE*, Las Vegas, USA, Jan. 2014, pp. 371–372.

[20] D. Umehara, H. Nishiyori, and Y. Morihiro, "Performance evaluation of CMFB transmultiplexer for broadband power line communications under narrowband interference," in *Proc. ISPLC*, Orlando, USA, Mar. 2006, pp. 50–55.

[21] A. Tonello and F. Pecile, "Efficient architectures for multiuser FMT systems and application to power line communications," *IEEE Trans. Commun.*, vol. 57, no. 5, pp. 1275–1279, May 2009.

[22] P. Odling, P. Borjesson, T. Magesacher, and T. Nordstrom, "An approach to analog mitigation of RFI," *IEEE J. Sel. Areas Commun.*, vol. 20, no. 5, pp. 974–986, Jun. 2002.

[23] D. Kang, S. Zhidkov, and H. Choi, "An adaptive detection and suppression of co-channel interference in DVB-T/H system," *IEEE Trans. Consum. Electron.*, vol. 56, no. 3, pp. 1320–1327, Aug. 2010.

- [24] J. Zhang and J. Meng, "Noise resistant OFDM for power-line communication systems," *IEEE Trans. Power Del.*, vol. 25, no. 2, pp. 693–701, Apr. 2010.
- [25] Y. Matsumoto, M. Takeuchi, K. Fujii, A. Sugiura, and Y. Yamanaka, "Performance analysis of interference problems involving DSSS WLAN systems and microwave ovens," *IEEE Trans. Electromagn. Compat.*, vol. 47, no. 1, pp. 45–53, Feb. 2005.
- [26] Y. Matsumoto, T. Shimizu, T. Murakami, K. Fujii, and A. Sugiura, "Impact of frequency-modulated harmonic noises from PCs on OFDM based WLAN systems," *IEEE Trans. Electromagn. Compat.*, vol. 49, no. 2, pp. 455–462, May 2007.
- [27] J. Corts, L. Dez, F. Caete, and J. Snchez-Martnez, "Analysis of the indoor broadband power-line noise scenario," *IEEE Trans. Electromagn. Compat.*, vol. 52, no. 4, pp. 849–858, 2010.
- [28] J. Tropp, "Just relax: convex programming methods for identifying sparse signals in noise," *IEEE Trans. Inf. Theory*, vol. 52, no. 3, pp. 1030–1051, Mar. 2006.
- [29] J. Tropp and A. Gilbert, "Signal recovery from random measurements via orthogonal matching pursuit," *IEEE Trans. Inf. Theory*, vol. 53, no. 12, pp. 4655–4666, Dec. 2007.
- [30] Y. Eldar and M. Mishali, "Robust recovery of signals from a structured union of subspaces," *IEEE Trans. Inf. Theory*, vol. 55, no. 11, pp. 5302–5316, Nov. 2009.
- [31] W. Dai and O. Milenkovic, "Subspace pursuit for compressive sensing signal reconstruction," *IEEE Trans. Inf. Theory*, vol. 55, no. 5, pp. 2230–2249, May 2009.
- [32] M. Zimmermann and K. Dostert, "A multipath model for the powerline channel," *IEEE Trans. Commun.*, vol. 50, no. 4, pp. 553–559, Apr. 2002.



Sicong Liu (S'15) received the B.S.E. degree in Electronic Engineering from Department of Electronic Engineering, Tsinghua University, Beijing, China. Currently, he is pursuing the Ph.D. degree in electronic engineering in the DTV Technology R&D Center, Department of Electronic Engineering, Tsinghua University.

His research interests lie in 5G wireless technologies, sparse signal processing and its applications on power line communications (PLC), smart grid communications, and noise and interference mitigation.



Fang Yang (M'11-SM'13) received the B.S.E. and Ph.D. degrees in electronic engineering from Tsinghua University, Beijing China, in 2005 and 2009, respectively.

Currently, he is an Associate Professor with the DTV Technology R&D Center, Tsinghua University. His research interests lie in the field of power line communication, visible light communication, and digital television terrestrial broadcasting.



Wenbo Ding (S'15) received his B.S.E degree (with distinction) in 2011 from the Department of Electronic Engineering in Tsinghua University, Beijing China. Currently, he is pursuing the Ph. D. degree at the DTV Technology R&D Center, Tsinghua University. His research interests lie in the

sparse signal processing and its applications in the field of the power line communication, visible light communication, smart

grid and future 5G wireless communications. He has published over 30 journal and conference papers. He has received IEEE Scott Helt Memorial Award for the best paper published in IEEE TRANSACTIONS ON BROADCASTING in 2015, the best paper award of the National Doctoral Student Academic Conference, the Tsinghua Top Grade Scholarship, and the Academic Star of Electronic Engineering Department in Tsinghua University in 2015.



Jian Song (M'06-SM'10-F'16) received his B. Eng and Ph. D. degrees in Electrical Engineering both from Tsinghua University, Beijing China in 1990 and 1995, respectively and worked for the same university upon his graduation. He has worked at The Chinese University of Hong Kong and University of

Waterloo, Canada in 1996 and 1997, respectively. He has been with Hughes Network Systems in USA for 7 years before joining the faculty team in Tsinghua in 2005 as a professor. He is now the director of Tsinghua's DTV Technology R&D center. He has been working in quite different areas of fiber-optic, satellite and wireless communications, as well as the power line communications. His current research interest is in the area of digital TV broadcasting.

He has published more than 200 peer-reviewed journal and conference papers. He holds 2 US and more than 40 Chinese patents. He is Fellow of both IEEE and IET.



Andrea M. Tonello (M'00-SM'02) received the Laurea degree (summa cum laude) and the PhD in electronics and telecommunications from the University of Padova, Italy, in 1996 and in 2003, respectively. From 1997 to 2002, he was with Bell Labs- Lucent Technologies, Whippany, NJ, USA, first as a Member of the

Technical Staff. Then, he was promoted to Technical Manager and appointed to Managing Director of the Bell Labs Italy division. In 2003, he joined the University of Udine, Italy, where he became Aggregate Professor in 2005 and Associate Professor in 2014.

Currently, he is Professor and Chair of the Embedded Communication Systems Group at the University of Klagenfurt, Klagenfurt, Austria. Dr. Tonello received several awards, including five best paper awards, the Bell Labs Recognition of Excellence Award (1999), the Distinguished Visiting Fellowship from the Royal Academy of Engineering, U.K. (2010), and the IEEE VTS Distinguished Lecturer Award (2011-2015). He is the Chair of the IEEE Communications Society Technical Committee on Power Line Communications. He is an Associate Editor of IEEE TRANSACTIONS ON COMMUNICATIONS and IEEE ACCESS. He was the General Chair of IEEE ISPLC 2011, IEEE SmartGridComm 2014 and the TPC Co-Chair of ISPLC 2007.